Renewable Energy 115 (2018) 926–930

Contents lists available at ScienceDirect

Renewable Energy

journal homepage: www.elsevier.com/locate/renene

On the time varying mitigation performance of reflective geoengineering technologies in cities

V. Lontorfos [a], C. Efthymiou [a], M. Santamouris [a, b, *]

[a] Physics Department, University of Athens, Greece
[b] The Anita Lawrence Chair of High Performance Architecture, Faculty of Built Environment, UNSW, Sydney, Australia

ARTICLE INFO

Article history:
Received 23 February 2017
Received in revised form
5 August 2017
Accepted 10 September 2017
Available online 10 September 2017

Keywords:
Urban heat island
Reflective cool materials
Ageing
Urban mitigation technologies

ABSTRACT

Cities face important overheating problems caused by the local and global climate change. Detailed mitigation and adaptation plans and strategies, are designed and applied to counterbalance the impact of the overheating challenges. Albedo management seems to be among the more considered mitigation strategies. A barrier to the wider use of reflecting technologies is the lack of quantitative experimental data and concrete knowledge about their mitigation contribution. Up to now, the performance of the reflective mitigation technologies is assessed based on simulation results considering the initial optical properties of the materials and neglecting ageing and weatherization phenomena. The article present information on the global performance of reflecting mitigation technologies, as measured in a large scale urban mitigation project employing several types of reflecting technologies. It is shown, that because of the weatherization effects, the mitigation potential of the materials is reduced, during the first year after their installation, by at least, 25%. Despite the ageing effects, reflective pavements have found to contribute in reducing the peak summer ambient temperature up to 1,7 K, while their surface temperature was up to 12,3 K lower than that of conventional pavement reducing considerably the sensible heat released to the atmosphere.

1. Introduction

The Urban Heat Island, is the most documented phenomenon of Climate Change. It refers, to the occurrence of increased urban ambient temperatures compared to the adjacent suburban and rural areas. The phenomenon, is the result of the positive thermal balance in cities caused by the increased absorption of the solar radiation, the release of anthropogenic heat, the change in land uses and the reduced heat losses, [1–3]. There are more than 400 cities in the world, where the existence of the Urban Heat Island is experimentally documented, [4–7]. The amplitude of the UHI may exceed 5 K and it varies as a function of the characteristics of the cities, the prevailing synoptic weather conditions, the experimental method used to assess the temperature distribution in the city and the selection of the so called reference station, [4]. Higher urban temperatures increase the peak electricity demand, the energy consumption for cooling, the concentration of harmful pollutants like the tropospheric ozone, deteriorate indoor and outdoor thermal comfort and has a significant impact on human health, [5,8]. From a global perspective, the UHI increases the peak electricity demand by 20 Watts per person and degree of temperature increase [9], while the average penalty on the energy demand for cooling induced by the urban heat island is close to 0.8 kWh per unit of city surface and degree of temperature increase, or 68 kWh per person and degree, [10]. Warming trends, adding together with the increase of the population, are expected to increase the stress on electricity demand for cooling throughout the 21 century and raise the consumption of the residential sector up to 750%, [11].

As a response to the serious urban overheating problems, several mitigation technologies, systems and techniques, such as the use of reflective materials for roofs and pavements, the use of additional urban greenery, the use of evaporative systems, and the heat dissipation to low temperature sinks, have been proposed for different climates, [12–14]. Advanced cool materials presenting a high solar reflectivity and thermal emissivity, are proposed as an alternative to decrease the absorption and storage of the solar heat in cities, and to reduce the sensible heat released to the atmosphere, [15]. Several technologies of reflective materials for roofs

* Corresponding author. The Anita Lawrence Chair of High Performance Architecture, Faculty of Built Environment, UNSW, Sydney, Australia.
E-mail address: m.santamouris@unsw.edu.au (M. Santamouris).

http://dx.doi.org/10.1016/j.renene.2017.09.033
0960-1481/

and pavements, have been designed and proposed, [16]. Based on their initial reflectivity value, most of the materials seem to present a considerable high mitigation potential. Reflective materials have been extensively used in roofs to decrease the cooling load of buildings. Research has shown that reflective roofs present a high energy efficiency. The ageing of weatherization problem of cool roofs is also well studied and important experimental information is available, [17,18]. Existing knowledge on the performance of reflective pavements is fully based on simulation studies performed using mesoscale or microclimatic models [19,20], while very limited experimental data from large scale applications is available, and usually do not account the performance loss because of the weatherization phenomena, [21]. Simulations of the expected temperature drop when cool materials are used in pavements and roofs, performed for 75 large scale mitigation projects around the globe, show that the average peak temperature drop achieved when cool roof technologies are used, is close to 1 K, increasing up to 1.3 K for the cool pavements and 1.43 K for the combination of cool roofs and pavements. The absolute maximum temperature drop is 2.3 K for the cool roofs, 2.5 K for the cool pavements and 3.4 K for their combination, [22]. It is also estimated that the decrease of the average and maximum temperature drop per 10% increase of the albedo is close to 0.27 K and 0.78 K, respectively, [22]. However, assessment of the real mitigation potential of reflective technologies should consider the optical ageing of the materials, and the possible decrease of their contribution and utilizability because of the interaction with other installed mitigation systems. Weatherisation of the reflecting materials due to the accumulation of dust, soot particles and biomass, exposure to ultraviolet radiation, microbial growth, moisture penetration and condensation, reduces considerably their initial solar reflectivity, [23,24]. A decrease of the solar reflectivity by 0.25, or 33% of the initial value, is measured after four years of exposure of the reflective materials, [25]. Large scale planning of mitigation policies in cities should be based on the real performance of reflective materials, and consider weatherization and other effects affecting the performance of reflective mitigation techniques.

This study, assess and present the real performance of albedo change technologies. The mitigation potential of reflecting materials, is reported, as measured and calculated on a large scale urban rehabilitation project, using almost 10,000 m^2 of cool pavements. The project refers to the rehabilitation of a large urban area in Athens, Greece and to our knowledge, it is among the largest mitigation projects employing reflecting mitigation technologies.

1.1. Description of the case study – measurements and simulations

The rehabilitation project is sited in the area of Athens, Greece in the municipality of Dafni-Ymittos and it concerns 3 squares and the corresponding routes that connect them in a conceivable axis of 5 km. The area suffers from a significant increase of the local ambient temperature and the amplitude of the urban heat island in the area exceeds 7 C, [26]. Rehabilitation works started in late 2012 and were completed in the fall of 2014. The former materials used in the area, were all conventional and rather degraded. The previous pavements were made of degraded asphalt, concrete and dark paving materials, presenting very low albedo varying from 0.04 to 0.22. About r 5170 m^2 of conventional concrete pavements and 4600 m^2 of bitumen pavements were replaced with materials of considerably higher reflectance. The reflectance of the concrete pavement has increased from 0.20 to 0.47 while the reflectance of the bitumen pavement increased from 0.04 to 0.26. Materials of moderate reflectivity are selected to avoid problems of glare and deterioration of the pedestrian comfort because of the reflected solar radiation and the corresponding increase of the mean radiant temperature, [27,28]. The new reflective pavements were developed adding Infrared reflective pigments in the mass of the concrete to increase their reflectivity in the near infrared spectrum. To increase the reflectivity of the bitumen pavements, transparent asphaltic resin and quartz chips from marble and granite were used in powder form. The spectral absorptivity of the pavements was measured using spectrophotometers, according to the ASTME903 (Figs. 1a and b), while reflectometers were also used to measure the in situ global albedo, according to ASTMC1549.

Extensive measurements were performed for seven continuous months to assess the instantaneous and global impact of the reflecting materials to the thermal balance of the area. it is designed and used a detailed experimental and theoretical protocol, involving the continuous monitoring of the main optical and thermal characteristics of the materials and also the measurement of the major climatic parameters in the area, before during and after the implementation of the reflecting. Climatic measurements were performed using a mobile monitoring station, energy bus, equipped with a folding antenna able to support sensors up to 20 m high. The mobile station travelled through the project area completing a specific route in a time interval of 1.5 h. The vertical distribution of the ambient temperature, wind speed and wind direction were measured, as well as the surface temperature in the whole area using infrared cameras. Stationary stations were also distributed in the area to monitor the ambient temperature and humidity on a continuous basis. All equipment was well calibrated and their accuracy is between 0.5 and 2%.

The thermal performance of the area was modelled using the microclimatic simulation software Envimet, [29]. The software is suitable for microclimatic studies, can predict the spatial distribution of the main climatic parameters and it is extensively validated, [30]. The software solves the Reynolds-averaged non hydrostatic Navier-Stokes equations for each grid in space and for each time step. Turbulence is calculated using the E-epsilon 1.5 order closure and the exchange coefficients in the air are calculated using the Prandtl-Kolmogorov relation. Air temperature and specific air humidity are determined by the different sources and sinks of sensible heat and vapor inside the model domain, involving vegetation, surfaces, façades and rooftops. Shortwave and longwave radiation are taken into account, including shading and reflections of different surfaces, building materials and complex geometries. The surface temperature and the distribution of soil temperature is calculated in 4 m depth with respect to the actual soil water content. An orthogonal Arakawa C-grid is used to represent the environment, so every building material must be approximated by grid points. The multitude of partial differential equations and other aspects in the model are solved by the Finite Difference Method. A partly implicit, partly explicit scheme is used depending on the subsystem analysed. In order to interpret the project area as best possible, the squares, the route axis, the neighbouring blocks as well as the vegetation were designed in the domain. Detailed profiles of albedo were obtained from the extensive measurements in the area and were selected as inputs for the various surfaces. The albedo of the cool coatings, has been taken into account in the model. Dimensions of the calculation grid are 219 m(χ) x 102 m(y) x 150.46 m(z) and it consists of 219 $\times$ 102 x 14 cells on each axis respectively. The real dimensions of the area that was simulated are 438 m(x) x 204 m(y) x 150.46 m(z) resulting in a spatial resolution of 2 to 1, while five nesting grids of total of 135 m were added in all 4 sides to ensure that flow fields are rightly calculated.

Researching the thermal impact of a real project is extremely difficult as it is not straight forward. Direct comparison of the pre-retrofit and the retrofitted state is not possible solemnly through the measurement data, as the boundary conditions in each case may be completely different.

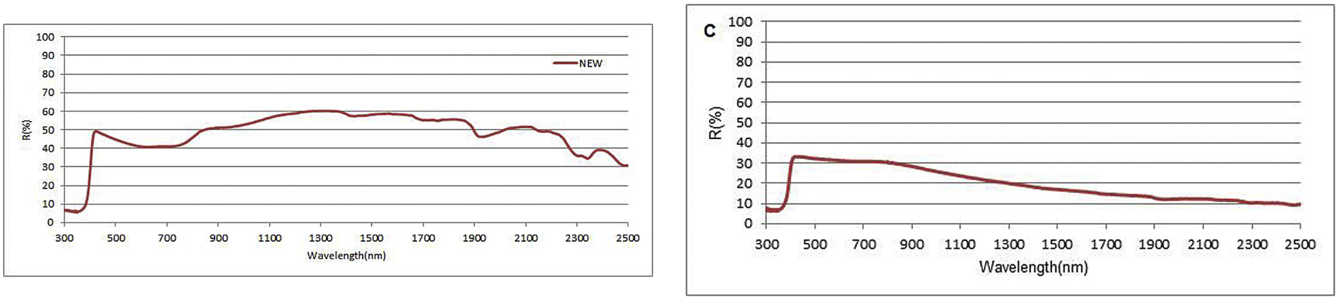

Fig. 1. (a). Spectral Reflectivity of the installed concrete pavements. (b): Spectral Reflectivity of the installed bitumen pavements.

The temperature distribution in the area, was simulated, before and during the whole experimental period, and the results were compared and validated against the corresponding measurements. In order to perform comparisons and assess the achieved temperature drop, the calibrated simulation model was used to normalize under the same climatic conditions, the results obtained under the various climatic and boundary conditions, before and during the experiment. The temperature drop in the area was calculated by comparing the results of two simulation sets, performed under the same climatic conditions, and for the prevailing boundary characteristics before and after the implementation of the reflecting materials, respectively. The potential decrease of the global mitigation potential of the area, caused by the optical degradation of the pavements, was assessed using the corresponding measured reflectivity values as inputs to the calibrated model.

In each calculation domain a comparison was made between the predicted and the measured values of both surface and ambient temperature in selected reference points. Reference data were deduced from the monitoring period performed before, during and after the rehabilitation of the area, therefore the evaluation refers to the pre and post-retrofit state of the area of interest. When a very good agreement between the modelled and measured values of the surface and the ambient temperatures was achieved, the final simulations were accepted. Fig. 2, shows the modelled and measured daily distribution of the surface temperature of the bitumen pavements for a typical day. The maximum difference between the predicted and measured surface temperature did not exceeded 0.3 C while for most of the time the difference was much lower. A very good agreement is also achieved between the predicted and the measured ambient temperature at 2 m height. Comparisons are performed for all measurement points and the maximum average daily difference did not exceed 0.5 K, while for most of the time the difference was much lower and inside the measurement errors. Boundary conditions and input climatic data remained the same in all the pre- and post-rehabilitation scenarios in order to be able to compare the corresponding results. The detailed measured albedo profiles, the area layout and the vegetation were altered to meet each state condition. The results of the normalized simulations were compared to calculate the achieved temperature drop in the area as well as the impact of the materials weatherization on the peak temperature drop. The followed calibration and normalization procedure permits to take benefit of all the detailed measurements performed and compare experimental results collected under different climatic and boundary conditions. A detailed error and sensitivity analysis was performed and it was identified that the maximum prediction error for the ambient temperature was ±0.25 C, and for the surface temperature ±0.1 C.

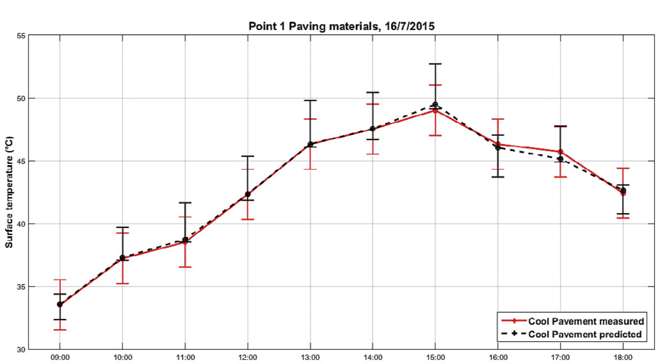

Fig. 2. Comparison of the predicted against the measured surface temperature of the bitumen pavement.

2. Results

The focus of the research was on the reduction of the ambient temperature, the decrease of the surface temperature in the area and the impact of the materials weatherization, on the potential drop of the ambient temperature. The results show that the peak ambient temperature drop is up to 1.7 ± 0.25 K. The estimation refers to the real performance of the materials during the end of the first year of operation and weatherization effects are taken into account, (Fig. 3). It is found that the peak ambient temperature drop occurs during the summer period and under synoptic weather conditions with high solar radiation, high ambient temperature and low wind speeds. Under sunny conditions, high advection rates decrease the surface temperature of both the conventional and reflecting pavements and limit the average ambient temperature drop down to 0.8 K. The maximum reduction of the ambient temperature occurs in summer and during the early afternoon hours while the range of the spatial change of the ambient temperature, is not exceeding 0.5 K. The minimum temperature drop during the summer period, is observed at night and it is close to 0.3 K. Under cloudy conditions during the day time, the ambient temperature drop is almost zero.

The results show that the surface temperature of the cool concrete pavements is reduced up to 12.3 K compared to the conventional pavements, while the surface temperature of the bitumen pavements is reduced up to 7.9 K. Measurements are performed under the actual conditions of the pavements and weatherisation effects were considered. Decreased surface temperatures contribute to reduce the sensible heat released to the atmosphere by the materials and fight the urban heat island. The maximum temperature drop was achieved in summer and in the early afternoon hours. During a summer day, the surface temperature drop of the concrete pavements varied between 4 K and 12.3 K, while the temperature drop during the night time was not exceeding 3 K. Correspondingly, the daytime, temperature reduction of the

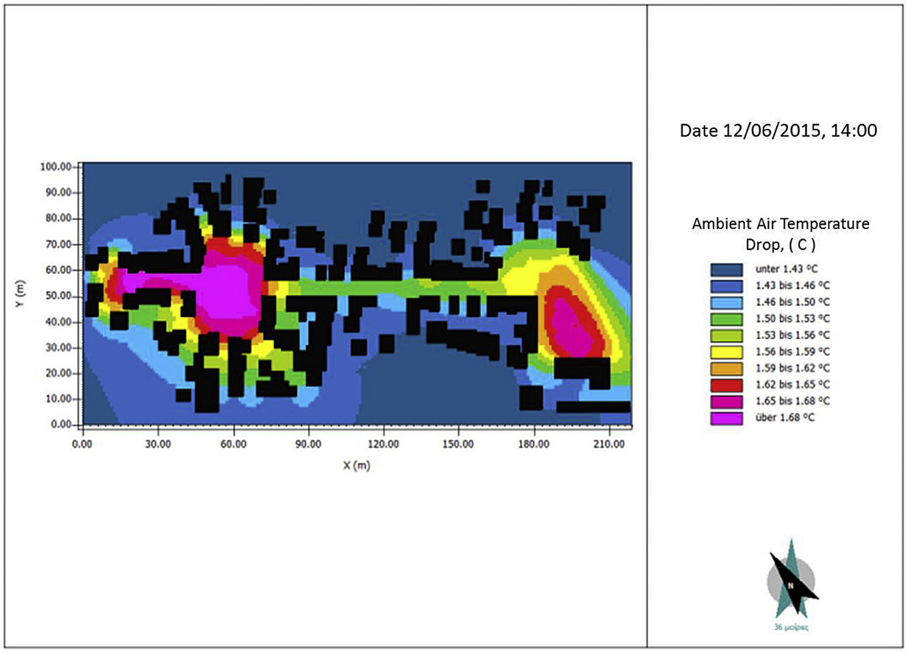

Fig. 3. Estimated Temperature Difference of the Ambient Temperature before and after the installation of the reflective materials.

bitumen pavements varied between 2 and 7.9 K, (Fig. 4).

A significant decrease of the reflectivity of both the concrete and bitumen pavements is observed as a function of time. A year after the installation of the pavements, the solar reflectivity of the concrete pavements was decreased from 0.47 to 0.40, while the reflectivity of the bitumen pavements was reduced from 0.26 to 0.15. It is observed that most of the reflectivity loss of the bitumen pavements occurred during the first month of their operation. Because of the important deposition of rubber on the surface of the pavements, from the tyres of cars, their reflectivity was reduced from 0.26 to 0.17 and then it was almost stabilized. The observed reflectivity loss of the concrete pavements was quite steady over time and was mainly due to the important deposition of dust on their surface. It is observed that pavements could recover part of the lost reflectivity when scrubbing them with wet solvents. It is estimated that the loss of the peak mitigation potential, because of the observed weatherization, was close to 0.5 K for the first year of the operation. It is estimated that the specific experimental results are in agreement with the prediction assessment proposed in Ref. [18], to assess the mitigation performance of cool pavements. According to this method, an increase of the local albedo by 0.25, results in a peak ambient temperature drop by 2.3 K. However, because of the weatherization phenomena, the real increase of the albedo was close to 0.17 and the average measured peak temperature drop was 1.7 K. About 200 questionnaires were distributed to the pedestrians to assess potential comfort problems because of the increased reflected solar radiation. Not particular concerns about thermal comfort conditions in the area were identified.

3. Discussion and conclusions

This is the first study that sheds light on the real mitigation potential of reflective pavements. The results show that the mitigation potential of reflecting technologies is important, and can contribute to counterbalance the effects of urban overheating. It is found that the wide application of reflecting pavements can reduce

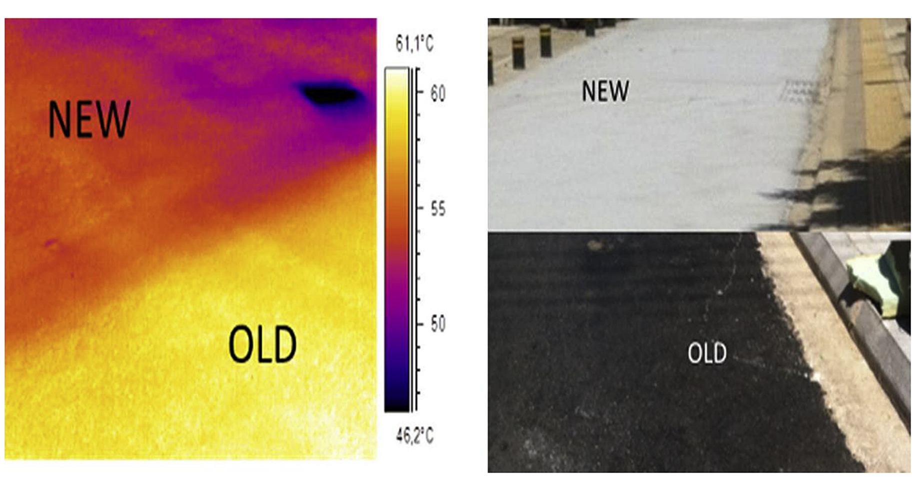

Fig. 4. Infrared Thermography of the asphaltic pavements before and after the rehabilitation.

the peak ambient temperature up to 1.7 K, despite the loss of efficiency caused by the ageing phenomena. It is verified experimentally, that the climatic impact of the reflecting pavements is higher during the hottest days of the year. The research found that the mitigation potential of reflecting materials is considerably reduced by weatherization and ageing phenomena. It is estimated that the loss of performance, during the first year of the project's operation, because of the ageing phenomena, may exceed 20–25%, of the initially estimated performance. It is also found that reflecting asphalt/bitumen pavements used in roads with car circulation, exhibit a strong loss of reflectivity, up to 40%, during the first period of operation. It is verified experimentally that under low wind speeds, the surface temperature of the reflecting pavements is up to 12.3 K lower that that of conventional pavements of the same color, despite the weatherization problems. Lower surface temperatures decrease the sensible heat released to the atmosphere, and contribute to enhance thermal comfort because of the lower emmited IR radiation. The impact of the increased reflected radiation on the pedestrian comfort was not studied in a systematic way, but no particular concerns about the comfort of the pedestrians were identified.

It is illustrated that reflective pavements contribute significantly to reduce the strength of urban heat island. However, in most places, the magnitude of the UHI exceeds 5 K, and despite the significant contribution of reflective pavements, additional mitigation technologies have to be applied. New advanced reflective technologies like the nanophotonic multilayer stacks of multiple optical materials [31], could contribute to achieve sub-ambient surface temperatures and enhance further the performance of reflecting technologies.

References

[1] Lei Zhao, Xuhui Lee, Ronald B. Smith, Keith Oleson, Strong contributions of local background climate to urban heat islands, Nature 511 (2014).
[2] M. Santamouris (Ed.), Energy and Climate in the Urban Built Environment, Routlege, London, 2007.
[3] T.R. Oke, G.T. Johnson, D.G. Steyn, I.D. Watson, Simulation of surface urban heat islands under ideal conditions at night. 2. Diagnosis of Causation, Bound. Layer Meteorol. 56 (1991) 339–358.
[4] M. Santamouris, Analyzing the heat island magnitude and characteristics in one hundred Asian and Australian cities and regions, Sci. Total Environ. 512–513 (2015) 582–598.
[5] M. Santamouris, Innovating to zero the building sector in Europe: minimising the energy consumption, eradication of the energy poverty and mitigating the local climate change, Sol. Energy 128 (2016) 61–94.
[6] Dana Taleb, Bassam Abu-Hijleh, Urban heat islands: potential effect of organic and structured urban configurations on temperature variations in Dubai, UAE, Renew. Energy 50 (2013) 747–762.
[7] Mehdi Shahrestani, Runming Yao, Zhiwen Luo, Erdal Turkbeyler, Hywel Davies, A field study of urban microclimates in London, Renew. Energy 73 (2015) 3–9.
[8] M. Santamouris, Regulating the damaged thermostat of the cities – status, impacts and mitigation strategies, energy and buildings, Energy Build. 91 (2015) 43–56.
[9] M. Santamouris, C. Cartalis, A. Synnefa, D. Kolokotsa, On the impact of urban heat island and global warming on the power demand and electricity consumption of buildings—a review, Energy Build. 98 (2015) 119–124.
[10] Santamouris, On the energy impact of urban heat island and global warming on buildings, Energy Build. 82 (2014) 100–113.
[11] M. Santamouris, Cooling of buildings. Past, present and future, Energy Build. 128 (2016) 617–638.
[12] H. Akbari, C. Cartalis, D. Kolokotsa, A. Muscio, A.L. Pisello, F. Rossi, M. Santamouris, A. Synnefa, N.H. Wong, M. Zinzi, Local climate change and urban heat island mitigation techniques – the state of the art, J. Civ. Eng. Manag. 22 (2016) 1–16.
[13] Stone Jr., Vargo Jason, Liu Peng, Habeeb Dana, DeLucia Anthony, Trail Marcus, Hu Yongtao, Russell Armistead, Avoided heat-related mortality through climate adaptation strategies in three US cities, PLos One 9 (6) (2014).
[14] M. Taleghani, David J. Sailor, Martin Tenpierik, Andy van den Dobbelsteen, Thermal assessment of heat mitigation strategies: the case of Portland, State University, Oregon, USA. Build. Environ. 73 (2014) 138–150.
[15] H. Akbari, M. Pomerantz, H. Taha, Cool surfaces and shade trees to reduce energy use and improve air quality in urban areas, Sol. Energy 70 (2001) 295–310.
[16] M. Santamouris, A. Synnefa, T. Karlessi, Using advanced cool materials in the urban built environment to mitigate heat islands and improve thermal comfort conditions, Sol. Energy 85 (2011) 3085–3102.
[17] Pisello Anna Laura, Santamouris Mattheos, Cotana Franco, Active cool roof effect : impact of cool roofs on cooling system efficiency, Adv. Build. Energy Res. 7 (2) (2013) 209–221.
[18] A.L. Pisello, V.L. Castaldo, G. Pignatta, F. Cotana, M. Santamouris, Experimental in-lab and in-field analysis of waterproof membranes for cool roof application and urban heat island mitigation, Energy Build. 114 (2016) 180–190.
[19] Y. Wang, Umberto Berardi, Hashem Akbari, Comparing the effects of urban heat island mitigation strategies for Toronto, Canada, Energy Build. 114 (2016) 2–19.
[20] H. Taha, Urban surface modification as a potential ozone air quality improvement strategy in California: a mesoscale modelling study, Boundary layer Meteorol. 127 (2008) 219–239.
[21] M. Santamouris, N. Gaitani, A. Spanou, M. Saliari, K. Gianopoulou, K. Vasilakopoulou, Using cool paving materials to improve microclimate of urban areas – design realisation and results of the flisvos project, Build. Environ. 53 (2012) 128–136.
[22] M. Santamouris, L. Ding, F. Fiorito, P. Oldfield, Paul Osmond, R. Paolini, D. Prasad, A. Synnefa, Passive and active cooling for the outdoor built environment – analysis and assessment of the cooling potential of mitigation technologies using performance data from 220 large scale projects, Sol. Energy (2017). Available online 19 December 2016, (in press).
[23] P. Berdahl, H. Akbari, L.S. Rose, Aging of reflective roofs: soot deposition, Appl. Opt. 41 (2002) 2355–2360.
[24] R. Levinson, P. Berdahl, A. Asefaw Berhe, H. Akbari, Effects of soiling and cleaning on the reflectance and solar heat gain of a light-colored roofing membrane, Atmos. Environ. 39 (2005) 7807–7824.
[25] E. Mastrapostoli, M. Santamouris, D. Kolokotsa, V. Perdikatsis, D. Venieri, K. Gobakis, On the aging of cool roofs. Measure of the optical degradation, chemical and biological analysis and assessment of the energy impact, Energy Build. 114 (2016) 191–199.
[26] I. Livada, M. Santamouris, K. Niachou, N. Papanikolaou, G. Mihalakakou, Determination of Places in the great Athens area where the heat island effect is observed, Theor. Appl. Climatol. 71 (2002) 219–230.
[27] Mohammad Taleghani, David Sailor, George A. Ban-Weiss, Micrometeorological simulations to predict the impacts of heat mitigation strategies on pedestrian thermal comfort in a Los Angeles neighborhood, Environ. Res. Lett. 11 (2016).
[28] B.H. Lynn, T.N. Carlson, C. Rosenzweig, R. Goldberg, L. Druyan, J. Cox, K. Civerolo, A modification to the NOAH LSM to simulate heat mitigation strategies in the New York city metropolitan area, J. Appl. Meteorol. Clim. 48 (2009) 199–216.
[29] M. Bruse, H. Fleer, Simulating surface-plant-air interactions inside urban environments with a three dimensional numerical model, Environ. Model. Softw. 13 (3–4) (1998) 373–384.
[30] M. Samaali, D. Courault, M. Bruse, A. Olioso, R. Occelli, Analysis of a 3D boundary layer model at local scale: validation on soybean surface radiative measurements, Atmos. Res. 85 (2007) 183–198.
[31] A.R. Gentle, G.B.A. Smith, Subambient open roof surface under the mid-summer sun, Adv. Sci. 2 (2015).